IEEE Access
Multidisciplinary | Rapid Review | Open Access Journal

Received April 4, 2020, accepted April 20, 2020, date of publication April 23, 2020, date of current version May 7, 2020.

Digital Object Identifier 10.1109/ACCESS.2020.2989931

Design of a Cyclic Shifted LACO-OFDM for Optical Wireless Communication

WEIWEN HU, (Member, IEEE)
Department of Electronic Engineering, Southern Taiwan University of Science and Technology, Tainan 710, Taiwan
e-mail: huweiwen1106@gmail.com

This work was supported in part by the Ministry of Science and Technology, Taiwan, under Grant MOST 107-2221-E-218-007-MY2.

ABSTRACT This paper proposes a cyclic shifted layer asymmetrically clipped optical orthogonal frequency division multiplexing system (CS-LACO-OFDM) for optical wireless communications. The transmitted signal in CS-LACO-OFDM is generated by combining the signal of the first layer and signals of the remaining L-1 layers with cyclic shift equivalents, where L is the number of the CS-LACO-OFDM layers. In particular, the sets of cyclic shift value in CS-LACO-OFDM are modulated on the odd subcarriers of the first layer with complex-valued symbols. Information on cyclic shift sets can be easily detected with the help of modulated symbols conveyed in the first layer without increasing the receiver complexity. Simulation results show that the CS-LACO-OFDM has a similar peak-to-average power ratio performance as LACO-OFDM with separate selective mapping scheme when the number of candidate signals is the same but at remarkably low computational complexity. Furthermore, the average bit error rate of CS-LACO-OFDM over all layers is minimized by the proposed optimal optical power allocation.

INDEX TERMS Hybrid modulation, peak-to-average power ratio, cyclic shift, visible light communication, layer asymmetrically-clipped optical orthogonal frequency division multiplexing.

I. INTRODUCTION

Compared with conventional radio frequency wireless communication system, orthogonal frequency division multiplexing (OFDM) based optical wireless communication (OWC) system is perceived as a promising technology that has numerous advantages, such as no electromagnetic interference, license-free spectrum, and high privacy protection [1]. The transmitted signals of OWC have to be real and unipolar owing to the inherent nature of an optical light emitting diode (LED) transmitter. To meet this criterion, pulse amplitude modulated discrete multitone (PAM-DMT), asymmetrically clipped optical OFDM (ACO-OFDM), flip OFDM, direct current-biased optical OFDM (DCO-OFDM) have been extensively discussed in the literature [2]–[6]. However, these schemes have some drawbacks. DCO-OFDM increases the transmitted optical power because of the introduction of DC-bias. Although PAM-DMT and ACO-OFDM achieve higher optical power efficiency than DCO-OFDM, the spectral efficiency is sacrificed by half. Moreover, flip OFDM transmits the positive and negative components of real bipolar OFDM signals over two frame durations at the cost of an additional transmission delay.

The associate editor coordinating the review of this manuscript and approving it for publication was Jie Tang.

Layer ACO-OFDM (LACO-OFDM) has been recently proposed for OWC systems, which combine different layers of conventional ACO-OFDM with different subcarriers [7]–[12]. Although LACO-OFDM enhances the spectral efficiency without adding DC-bias, LACO-OFDM continues to suffer from the non-linear signal distortion of LED because of the presence of a high peak-to-average power ratio (PAPR). The high PAPR problems have been addressed by numerous PAPR reduction schemes for OFDM-based OWC systems [13]–[20]. However, these PAPR reduction schemes may be unsuitable for LACO-OFDM because of the specific superimposed properties of transmitted signals. The majority of these methods also require high computational complexity. To the best of the author's knowledge, the design of the low-PAPR transmitter with low complexity for LACO-OFDM has yet to be addressed sufficiently.

Inspired by the joint design of low-PAPR and low-complexity in a LACO-OFDM system, a cyclic shifted LACO-OFDM (CS-LACO-OFDM) is proposed for OWC. At the transmitter side of the CS-LACO-OFDM, the signal with the lowest PAPR is chosen to be transmitted from the combination of the signal of the first layer and the signals of the remaining L-1 layers with cyclic shift equivalents. In particular, the sets of cyclic shift value in CS-LACO-OFDM are encoded into binary bits and modulated on the odd

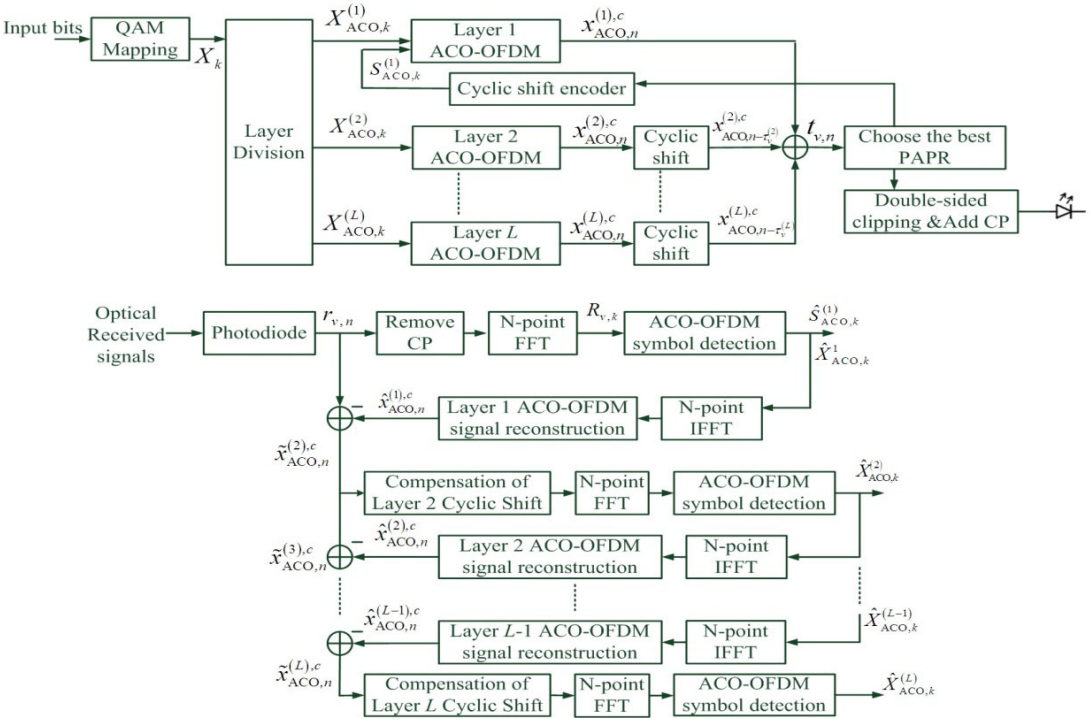

FIGURE 1. Transmitter and receiver of CS-LACO-OFDM.

subcarriers of the first layer with complex-valued symbols. At the receiver, the CS-LACO-OFDM symbols on the first layer are first demodulated as in LACO-OFDM, and the information on cyclic shift sets can also be detected with the assistance of the modulated symbols transmitted in the first layer. Thereafter, the CS-LACO-OFDM symbols on the remaining high L-1 layers can be demodulated layer-by-layer without increasing the receiver complexity. The main contributions of the CS-LACO-OFDM system are listed as follows.

1) In terms of the optical modulation for OWC systems, this is the first joint design of the low-PAPR and low-complexity in a LACO-OFDM system.

2) Compared with the SLM-based scheme that was applied to each layer of LACO-OFDM, CS-LACO-OFDM achieves considerable PAPR reduction performance, but at substantially low computational complexity. Furthermore, the CS-LACO-OFDM system has the same receiver complexity as that of LACO-OFDM.

3) We also propose the optimal optical power allocation to improve the detection performance of the sets of cyclic shift and minimize the average bit error rate of CS-LACO-OFDM over all the layers.

II. PROPOSED CS-LACO-OFDM

This section illustrates the transmitter architecture, receiver architecture, optimal optical power allocation, and complexity analysis in detail.

A. TRANSMITTER ARCHITECTURE OF CS-LACO-OFDM

The upper part of Fig. 1 illustrates the block diagrams of the CS-LACO-OFDM transmitter. Similar to LACO-OFDM, CS-LACO-OFDM divides the modulated symbols into L single-layer ACO-OFDM modulators, where each ACO-OFDM modulator transforms the frequency-domain ACO-OFDM symbols into the clipped time-domain ACO-OFDM signals by applying N-point inverse fast Fourier transform (IFFT) operations with Hermitian symmetry and asymmetrically clipping. In general, we assume that the ACO-OFDM symbols of the lth layer are independently chosen from the QAM constellation $M^{(l)}$ with zero mean and variance of σ^2. Therefore, the time-domain ACO-OFDM signals of the lth layer is provided as follows:

$$x_{\mathrm{ACO},n}^{(l)} = \frac{1}{\sqrt{N}} \sum_{k=0}^{N-1} X_{\mathrm{ACO},k}^{(l)} e^{j2\pi nk/N}, \quad 0 \le n \le N-1, \tag{1}$$

where $1 \le l \le L, X_{\mathrm{ACO},k}^{(l)} = \left(X_{\mathrm{ACO},N-k}^{(l)}\right)^*$ and $X_{\mathrm{ACO},k}^{(l)}$ is the kth subcarrier in the lth layer. In CS-LACO-OFDM, the modulated subcarriers for the lth layer are provided as follows:

$$\mathbf{X}_{\mathrm{ACO}}^{(l)} = \begin{cases} X_{\mathrm{ACO},k}^{(l)}, & k = \Omega_l \\ 0, & \text{otherwise}, \end{cases} \tag{2}$$

where $\Omega_l = \left\{2^{l-1}, 3\times 2^{l-1}, 5\times 2^{l-1}, \ldots, N-2^{l-1}\right\}$ denotes the sets of Layer l subcarriers carrying data. As shown in [10], $x_{\mathrm{ACO},n}^{(l)}$ is a real-valued bipolar signal that has an anti-symmetry as follows:

$$x_{\mathrm{ACO},n}^{(l)} = -x_{\mathrm{ACO},n+N/2^l}^{(l)}, \quad 0 \le n \le N\Big/2^l - 1. \tag{3}$$

In addition, the variance of $x_{\mathrm{ACO},n}^{(l)}$ for the lth layer is provided as follows:

$$E\left[\left|x_{\mathrm{ACO},n}^{(l)}\right|^2\right] = \sigma^2 \Big/ 2^l. \tag{4}$$

Thereafter, the negative amplitude of $x_{\mathrm{ACO},n}^{(l)}$ has to be clipped to produce unipolar signals, which are suitable for transmission in optical wireless channel. The generated unipolar signals for the lth layer are denoted as follows:

$$x_{\mathrm{ACO},n}^{(l),c} = \frac{1}{2}\left(x_{\mathrm{ACO},n}^{(l)} + \left|x_{\mathrm{ACO},n}^{(l)}\right|\right) = \begin{cases} x_{\mathrm{ACO},n}^{(l)}, & x_{\mathrm{ACO},n}^{(l)} \geq 0 \\ 0, & x_{\mathrm{ACO},n}^{(l)} < 0. \end{cases} \tag{5}$$

Compared with LACO-OFDM, the transmitted signal in the CS-LACO-OFDM is obtained by combining the clipped Layer 1 ACO-OFDM signal and the cyclic shift version of the clipped Layer l ($l \geq 2$) ACO-OFDM signal. Therefore, the vth combined CS-LACO-OFDM signal can be obtained as follows:

$$t_{v,n} = \rho^{(1)} \cdot x_{\mathrm{ACO},n}^{(1),c} + \sum_{l=2}^{L} \rho^{(l)} \cdot x_{\mathrm{ACO},n-\tau_v^{(l)}}^{(l),c}, \tag{6}$$

where $0 \leq v \leq V-1$, $\rho^{(l)}$ is the optical power allocation factor to the lth layer and $\tau_v^{(l)}$ is the cyclic shift in the Layer l ACO-OFDM of the vth transmitted signal. The lth layer ACO-OFDM signal with cyclic shift $\tau_v^{(l)}$ is defined as follows:

$$\begin{aligned} &x_{\mathrm{ACO},n-\tau_v^{(l)}}^{(l),c} \\ &= [x_{\mathrm{ACO},\tau_v^{(l)}}^{(l),c}, \ldots, x_{\mathrm{ACO},N-1}^{(l),c}, x_{\mathrm{ACO},0}^{(l),c}, \ldots, x_{\mathrm{ACO},\tau_v^{(l)}-1}^{(l),c}]. \end{aligned} \tag{7}$$

The current study denotes $\tau_v = \left\{0, \tau_v^{(2)}, \tau_v^{(3)}, \ldots, \tau_v^{(L)}\right\}$ as a cyclic shift set for the vth transmitted signal. The CS-LACO-OFDM signal with the lowest PAPR among the V alternative cyclic shift sets is determined and transmitted as follows:

$$\hat{v} = \arg \min_{0 \leq v \leq V-1} \mathrm{PAPR}\left(t_{v,n}\right), \tag{8}$$

where PAPR of $t_{v,n}$ in CS-LACO-OFDM is defined as follows:

$$\mathrm{PAPR}\left(t_{v,n}\right) = \frac{\max\limits_{0 \leq n \leq N-1} \left|t_{v,n}\right|^2}{E\left[\left|t_{v,n}\right|^2\right]}. \tag{9}$$

Lastly, the transmitted signal suffers from the double-sided clipping of LED, where the resultant signal is provided as follows:

$$t_{\hat{v},n} = \begin{cases} v_{upper}, & t_{v,n} \geq v_{upper} \\ t_{\hat{v},n}, & v_{ton} < t_{v,n} < v_{upper} \\ v_{ton}, & t_{v,n} \leq v_{ton}, \end{cases} \tag{10}$$

where v_{upper} and v_{ton} denote the maximum permissible and turn-on voltages, respectively. In a CS-LACO-OFDM system, the V cyclic shift sets have to be modulated to complex-valued symbols based on the selected constellation and assigned thereafter on the odd subcarriers of the first layer. The number of required odd subcarriers is calculated as $N_{cyclic} = \left\lceil \log_2 V \Big/ \log_2 M^{(1)} \right\rceil$, where $\lceil \kappa \rceil$ is the ceiling function that gives the smallest integer $\geq \kappa$, and $M^{(1)}$ is the constellation set of the first layer. Evidently, CS-LACO-OFDM only requires the N_{cyclic} subcarriers of the first layer to indicate the selected signal without losing considerable spectrum efficiency. Accordingly, the modulated subcarriers of the first layer are modified as follows:

$$\begin{aligned} &\mathbf{X}_{\mathrm{ACO}}^{(1)} \\ &= \begin{cases} S_{\mathrm{ACO},k}^{(1)}, & k = 1, 3, \ldots, 2N_{cyclic} - 1 \\ X_{\mathrm{ACO},k}^{(1)}, & k = 2N_{cyclic}+1, 2N_{cyclic}+3, \ldots, N/2-1. \end{cases} \end{aligned} \tag{11}$$

B. RECEIVER ARCHITECTURE OF CS-LACO-OFDM

The proposed receiver architecture of CS-LACO-OFDM is illustrated in the bottom part of Fig. 1. The received electrical signal is obtained from the output of photodiode and is expressed as $r_{v,n} = h_n \otimes t_{\hat{v},n} + w_n$, where h_n is the channel impulse frequency, $\otimes$ denotes the circular convolution, and w_n is time-domain AWGN noise with a zero mean and a variance of σ_w^2. After removing the cyclic prefix and applying N-point FFT on the received electrical signal, the resulting frequency-domain symbols are obtained as $R_{v,k} = H_k T_{v,k} + W_k$, where H_k is the channel frequency response of the kth subcarrier. Based on the fact that the clipping noise of Layer 1 ACO-OFDM only impacts even subcarriers, the Layer 1 ACO-OFDM symbols could be first estimated using the odd subcarriers of $R_{v,k}$:

$$\begin{aligned} \hat{Y}_k &= \arg \min_{X_k \in M^{(1)}} \left|\frac{2R_{v,k}}{H_k} - X_k\right| \\ &= \begin{cases} \hat{S}_{\mathrm{ACO},k}^{(1)}, & k = 1, 3, \ldots, 2N_{cyclic} - 1 \\ \hat{X}_{\mathrm{ACO},k}^{(1)}, & k = 2N_{cyclic}+1, 2N_{cyclic}+3, \ldots, N/2-1, \end{cases} \end{aligned} \tag{12}$$

where $M^{(1)}$ is the constellation set of the Layer 1 ACO-OFDM symbols. As shown in (12), before demodulating ACO-OFDM symbols in the high layer, we should compensate the cyclic shift of each layer based on the estimated symbol $\hat{S}_{\mathrm{ACO},k}^{(1)}$. It means that information on cyclic shift sets can be easily detected with the help of modulated symbols conveyed in the first layer without increasing the receiver complexity. Subsequently, the time-domain regenerated Layer 1 ACO-OFDM signals $\hat{x}_{\mathrm{ACO},n}^{(1),c}$ are obtained using equations (1) and (5). The channel frequency response could be obtained through channel estimation and is assumed to be a perfect estimation in this paper. Accordingly, the estimated Layer 2 ACO-OFDM signals can be obtained by subtracting the time-domain regenerated Layer 1 ACO-OFDM signals from the received signals

with the channel compensation:

$$\begin{aligned}
&\tilde{x}^{(2),c}_{\mathrm{ACO},n} \\
&= r_{v,n} - \rho^{(1)}\hat{x}^{(1),c}_{\mathrm{ACO},n} \\
&= t_{\hat{v},n} + w_n - \rho^{(1)}\hat{x}^{(1),c}_{\mathrm{ACO},n} \\
&= \rho^{(1)} \cdot x^{(1),c}_{\mathrm{ACO},n} + \sum_{l=2}^{L} \rho^{(l)} x^{(l),c}_{\mathrm{ACO},n-\tau_v^{(l)}+\tau_{\hat{v}}^{(l)}} - \rho^{(1)}\hat{x}^{(1),c}_{\mathrm{ACO},n} + w_n \\
&= \rho^{(1)}\left(x^{(1),c}_{\mathrm{ACO},n} - \hat{x}^{(1),c}_{\mathrm{ACO},n}\right) + \sum_{l=2}^{L} \rho^{(l)} x^{(l),c}_{\mathrm{ACO},n-\tau_v^{(l)}+\tau_{\hat{v}}^{(l)}} + w_n \\
&= \rho^{(1)} c^{(1)}_{\mathrm{ACO},n} + \sum_{l=2}^{L} \rho^{(l)} x^{(l),c}_{\mathrm{ACO},n-\Delta_{\hat{v}}^{(l)}} + w_n, \qquad (13)
\end{aligned}$$

where $c^{(1)}_{\mathrm{ACO},n} = \left(x^{(1),c}_{\mathrm{ACO},n} - \hat{x}^{(1),c}_{\mathrm{ACO},n}\right)$ and $\Delta_{\hat{v}}^{(l)} = \tau_v^{(l)} - \tau_{\hat{v}}^{(l)}$ denotes the estimation error of the Layer 1 ACO-OFDM symbol and cyclic shift of the lth layer. After applying the N-point FFT operation on (13), we could obtain the frequency-domain Layer 2 ACO-OFDM symbols as follows:

$$\begin{aligned}
&\tilde{X}^{(2),c}_{\mathrm{ACO},k} \\
&= \frac{1}{2}\rho^{(2)} X^{(2)}_{\mathrm{ACO},k} e^{j2\pi k\Delta_l/N} + \frac{1}{2}\rho^{(2)} I^{(2)}_{\mathrm{ACO},k} e^{j2\pi k\Delta_l/N} \\
&\quad + U^{(l)}_{\mathrm{ACO},k} + \rho^{(1)} C^{(1)}_{\mathrm{ACO},k} + W_{\mathrm{ACO},k}, \qquad (14)
\end{aligned}$$

where $I^{(2)}_{\mathrm{ACO},k}, U^{(l)}_{\mathrm{ACO},k}, C^{1}_{\mathrm{ACO},k}, W_{\mathrm{ACO},k}$ denote the clipping noise of the Layer 2 ACO-OFDM symbol, frequency-domain interference from the high layer of the ACO-OFDM symbols, estimation error of the Layer 1 ACO-OFDM symbol, and AWGN noises, respectively, which are provided as follows:

$$I^{(2)}_{\mathrm{ACO},k} = \sum\nolimits_{n=0}^{N-1} \left|x^{(2)}_{\mathrm{ACO},n}\right| \cdot e^{-j2\pi kn/N}, \qquad (15)$$

$$U^{(l)}_{\mathrm{ACO},k} = \sum\nolimits_{n=0}^{N-1} \left(\sum_{l=3}^{L} \rho^{(l)} \cdot x^{(l),c}_{\mathrm{ACO},n-\Delta_l}\right) \cdot e^{-j2\pi kn/N}, \qquad (16)$$

$$C^{1}_{\mathrm{ACO},k} = \sum_{n=0}^{N-1} c^{(1)}_{\mathrm{ACO},n} \cdot e^{-j2\pi kn/N}, \qquad (17)$$

At high SNR, $c^{(1)}_{\mathrm{ACO},n} \approx 0$ and $\Delta_l = 0$, Equation (14) could be further simplified as follows:

$$\tilde{X}^{(2),c}_{\mathrm{ACO},k} \approx \frac{1}{2}\rho^{(2)} X^{(2)}_{\mathrm{ACO},k} + \frac{1}{2}\rho^{(2)} I^{(2)}_{\mathrm{ACO},k} + W_{ACO,k}. \qquad (18)$$

where $U^{(l)}_{\mathrm{ACO},k} = 0$ depends on the fact that the carriers used in each ACO-OFDM layer do not overlap, and the demodulation of the low layer is unaffected by the high layers. Therefore, the Layer 2 ACO-OFDM symbols could be estimated as follows:

$$\hat{X}^{(2)}_{\mathrm{ACO},k} = \arg\min_{X_k \in M^{(2)}} \left|2\tilde{X}^{(2),c}_{\mathrm{ACO},k} - X_k\right|, \qquad (19)$$

where $k \in \Omega_2 = \{2, 6, \ldots, N-2\}$ and $M^{(2)}$ is the constellation set of the Layer 2 ACO-OFDM symbols. Thereafter, the ACO-OFDM symbols in the high layers could be estimated successively in similar fashion as follows:

$$\hat{X}^{(l)}_{\mathrm{ACO},k} = \arg\min_{X_k \in M^{(l)}} \left|2\tilde{X}^{(l),c}_{\mathrm{ACO},k} - X_k\right|, k \in \Omega_l. \qquad (20)$$

C. OPTIMIZATION OF THE OPTICAL POWER ALLOCATION

In CS-LACO-OFDM systems, each layer can modulate different subcarriers with different optical power allocation. Without loss of generality, we assume that each layer uses the same modulation schemes, the constellation sets of which are denoted as $M^{(l)} = M, 1 \le l \le L$. As derived in [12], BER of the Layer 1 ACO-OFDM symbols is given as follows:

$$B_1 = \frac{4\left(\sqrt{M}-1\right)}{\sqrt{M}\log_2(M)} Q\left(\sqrt{\frac{3}{M-1} \cdot \frac{E_{s,1}}{N_o}}\right), \qquad (21)$$

where $E_{s,1}/N_o$ is the electrical energy-per-bit to noise power spectral density of the Layer 1 ACO-OFDM symbols. Thus, BER of the Layer 2 ACO-OFDM symbols could be derived as follows:

$$\begin{aligned}
B_2 &= B_1 \cdot B_{2|\bar{1}} + (1 - B_1) \cdot B_{2|1} \\
&= B_{2|1} + B_1\left(B_{2|\bar{1}} - B_{2|1}\right), \qquad (22)
\end{aligned}$$

where $B_{2|1}$ and $B_{2|\bar{1}}$ denote the conditional probability of the Layer 2 ACO-OFDM signals error, given that Layer 1 ACO-OFDM signals have been demodulated successfully and wrongly, respectively. In general, $B_{2|\bar{1}}$ and $B_{2|1}$ could be small under high SNR. Thus, Equation (22) is approximately obtained as follows:

$$B_2 \approx B_{2|1} = \frac{4\left(\sqrt{M}-1\right)}{\sqrt{M}\log_2(M)} Q\left(\sqrt{\frac{3}{M-1} \cdot \frac{E_{s,2}}{N_o}}\right). \qquad (23)$$

BER of the high layer ACO-OFDM symbols relies on the estimation of the low layers. Thus, the BER performance of the lth layer ACO-OFDM is obtained as follows:

$$B_l \approx B_{l|1\sim l-1} = \frac{4\left(\sqrt{M}-1\right)}{\sqrt{M}\log_2(M)} Q\left(\sqrt{\frac{3}{M-1} \cdot \frac{E_{s,l}}{N_o}}\right). \qquad (24)$$

Given the Hermitian symmetry on the lth ACO-OFDM, only the $N/2^{l+1}$ subcarriers are used to modulate the ACO-OFDM symbols. Thus, the overall average BER for the L layers is expressed as follows:

$$B_{avg} = \frac{\sum_{l=1}^{L} \frac{N}{2^{l+1}} \cdot \log_2 M \cdot B_l}{\sum_{l=1}^{L} \frac{N}{2^{l+1}} \cdot \log_2 M}. \qquad (25)$$

The object of this study is to find the optimal optical power allocation on each layer to minimize the average BER performance as follows:

$$\begin{aligned}
\left\{\rho^{(1)}, \rho^{(2)}, \ldots, \rho^{(L)}\right\} &= \arg\min_{\rho^{(l)}, 1\le l\le L} B_{avg}, \\
&\text{subject to } E\left[t_{v,n}\right] = 1. \qquad (26)
\end{aligned}$$

The average BER performance is highly relevant to optical power allocation, side information detection, and adopted modulation constellation set. The electrical power of the Layer l clipped ACO-OFDM signals has been verified and calculated as follows:

$$E\left[\left|x_{\mathrm{ACO},n}^{(l),c}\right|^2\right] = \sigma^2 \Big/ 2^{l+1}. \tag{27}$$

Moreover, the optical power of the Layer l ACO-OFDM signals is also easily proven as follows:

$$E\left[x_{\mathrm{ACO},n}^{(l),c}\right] = \sigma \Big/ \left(\sqrt{2^l} \cdot \sqrt{2\pi}\right). \tag{28}$$

The minimal average BER performance can be achieved on the bases of these observations, in which each subcarrier of the lth layer should have equal electrical power. Thus, the optical power allocation to the lth layer ACO-OFDM signals can be derived as follows:

$$\rho^{(l)} = \frac{1}{\left(\sqrt{2}\right)^{l-1}} \cdot \frac{2\left(\sqrt{2}\right)^{L} - \left(\sqrt{2}\right)^{L+1}}{2\left(\sqrt{2}\right)^{L} - 2}. \tag{29}$$

D. ANALYSIS OF COMPUTATIONAL COMPLEXITY

On the basis of Equation (6), the candidate signals of a CS-LACO-OFDM system are constructed in the time domain, while the conventional SLM (CSLM) scheme generates the candidate signals in the frequency domain. For a fair comparison, we analyze the overall computational complexity in terms of the number of real multiplications and real additions required in the time-domain and frequency-domain operations. Moreover, we exclude the computational complexity of calculation of PAPR because all schemes have the same complexity. Given that the number of candidate signal is V, we assume that Layer 1 ACO-OFDM signal is unchanged and Layer $l (l \geq 2)$ ACO-OFDM signal is multiplied component-wise with the same phase sequence when the CSLM scheme is applied to the CS-LACO-OFDM system. Therefore, the CSLM scheme requires the VL IFFT operations with the V candidate signals. Each N-point IFFT notably needs the $2N \log_2 N$ real multiplications and $3N \log_2 N$ real additions. Moreover, the additional $(L-1)N$ real additions are needed to combine the L-Layer ACO-OFDM time-domain signals. Therefore, the total computational complexities required in the CSLM scheme are $3VLN \log_2 N + V(L-1)N$ real additions and $2VLN \log_2 N$ real multiplications, respectively.

A CS-LACO-OFDM system only needs the L IFFT operations to generate the L-Layer ACO-OFDM signals and requires $(L-1)N$ real additions to combine all L-Layer time-domain ACO-OFDM signals. Therefore, the total computational complexities required in CS-LACO-OFDM are $3LN \log_2 N + V(L-1)N$ real additions and $2LN \log_2 N$ real multiplications, respectively. To explain the improvement on the computational complexity by the CS-LACO-OFDM system, we define the computational complexity reduction ratio (CCRR) as follows:

$$\mathrm{CCRR} = \left(1 - \frac{\text{complexity of the CS-LACO-OFDM}}{\text{complexity of the conventional schemes}}\right) \times 100\%. \tag{30}$$

We can easily obtain CCRR regarding real multiplications and real additions, denoted by CCRR_{rm} and CCRR_{ra}, respectively, as follows:

$$\mathrm{CCRR}_{rm} = \left(1 - \frac{2LN \log_2 N}{2VLN \log_2 N}\right) \times 100\% = \left(1 - \frac{1}{V}\right) \times 100\%. \tag{31}$$

$$\begin{aligned}\mathrm{CCRR}_{ra} &= \left(1 - \frac{3LN \log_2 N + V(L-1)N}{3VLN \log_2 N + V(L-1)N}\right) \times 100\% \\ &= \left(\frac{3LN \log_2 N (V-1)}{3VLN \log_2 N + V(L-1)N}\right) \times 100\%.\end{aligned} \tag{32}$$

Evidently, equations (31) and (32) show that CS-LACO-OFDM can achieve the high CCRR in real multiplications and real additions when V increases. The numerical analysis provided in Table 1 is consistent with the mentioned above.

III. SIMULATION RESULTS

This section evaluates the performance of the CS-LACO-OFDM system in terms of the average BER and complementary cumulative distribution function (CCDF) of PAPR by simulations. We consider the 6-Layer ACO-OFDM with 128 subcarriers ($N = 128$ and $L = 6$), where the symbols are modulated with 16-QAM in all layers and the optical power allocation for each layer is obtained from equation (29).

The indicators of cyclic shift sets in the CS-LACO-OFDM system are modulated on the odd subcarriers of the first layer with the complex-valued symbols. Thus, we should first decode the Layer 1 ACO-OFDM signal to extract the information of the cyclic shift sets. Fig. 2 shows the detection error rate of cyclic shift sets with the proposed optical power allocation and the equal optical power allocation when the adopted subcarriers N_{cyclic} are QPSK and 16QAM modulation, respectively. In this figure, 16 candidate signals are adopted leading to the required subcarriers of two and one for QPSK and 16QAM, respectively. Evidently, the proposed power allocation outperforms the equal power allocation by a SNR reduction of 7dB and 5dB for QPSK and 16QAM, respectively, at a target of detection error rate of 10^{-3}.

Fig. 3 shows CCDF of PAPR for the CS-LACO-OFDM, 6-Layer ACO-OFDM with SLM scheme, and 6-Layer ACO-OFDM without PAPR reduction. In this figure, the optimal power allocation is used in all schemes. CS-LACO-OFDM has a similar PAPR performance as 6-Layer ACO-OFDM with the SLM scheme when the

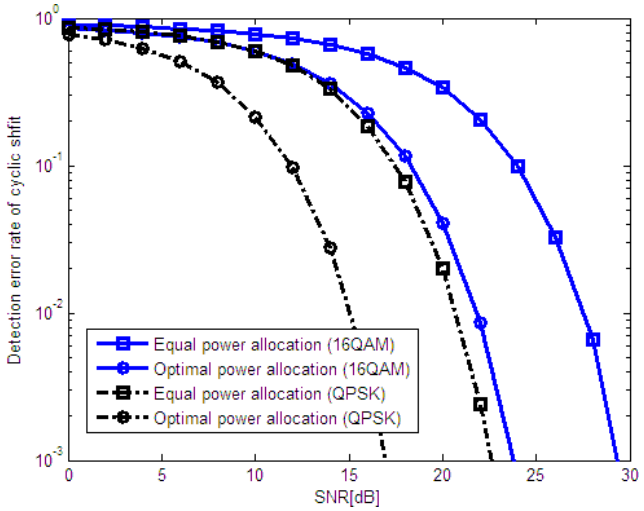

FIGURE 2. Detection error rate of the cyclic shift sets with equal and optimal power allocation.

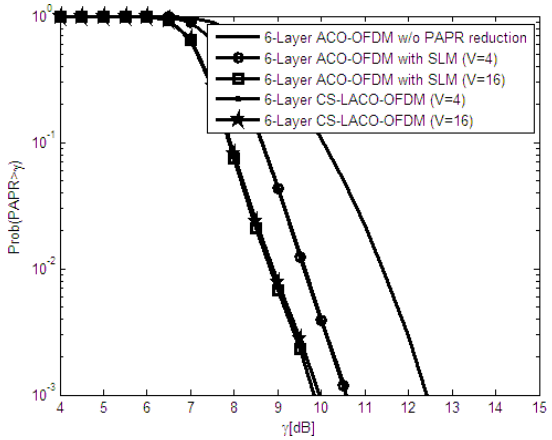

FIGURE 3. CCDF curves of PAPR for different schemes.

TABLE 1. CCRRs of the CS-LACO-OFDM over the CSLM scheme.

	N = 128, V = 4		N = 128, V = 16	
	$CCRR_{rm}$	$CCRR_{ra}$	$CCRR_{rm}$	$CCRR_{ra}$
L = 1	75%	75%	93.75%	93.75%
L = 2	75%	73.26%	93.75%	91.57%
L = 3	75%	72.69%	93.75%	90.87%
L = 4	75%	72.41%	93.75%	90.52%
L = 5	75%	72.25%	93.75%	90.31%
L = 6	75%	72.14%	93.75%	90.17%

number of candidate signals is the same, but at a remarkably lower computational complexity as shown in Table 1.

Fig. 4 shows the average BER of the 16-QAM modulation 6-Layer CS-LACO-OFDM system using equal power allocation and the proposed power allocation. The BER performance of LACO-OFDM with conventional SLM schemes and perfect side information is also shown in this figure as the benchmark. Note that from the simulation results that the average BER performance of CS-LACO-OFDM is close to the LACO-OFDM with SLM when the optimal optical power allocation is used. However, a marginal gap exists

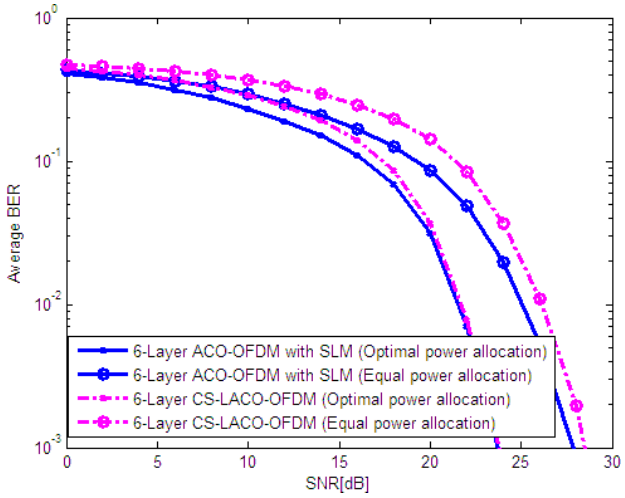

FIGURE 4. Average BER curves for different schemes.

in the average BER performance of CS-LACO-OFDM and LACO-OFDM with SLM under the equal power allocation. The reason is that the detection error rate of the cyclic shift sets with the equal power allocation is worse than that of the proposed optical power allocation.

IV. CONCLUSION

This study proposed a cyclic shifted layer asymmetrically clipped optical orthogonal frequency division multiplexing system for optical wireless communications. The proposed system has a similar PAPR performance as LACO-OFDM with separate SLM scheme when the number of candidate signals is the same, but at a remarkably lower computational complexity. Compared with equal power allocation scheme, the proposed optimal optical power allocation could achieve an improved performance in terms of the detection of cyclic shift sets and average BER over all layers.

REFERENCES

[1] H. Chen and Z. Xu, "A two-dimensional constellation design method for visible light communications with signal-dependent shot noise," *IEEE Commun. Lett.*, vol. 22, no. 9, pp. 1786–1789, Sep. 2018.
[2] Z. Wang, Q. Wang, S. Chen, and L. Hanzo, "An adaptive scaling and biasing scheme for OFDM-based visible light communication systems," *Opt. Express*, vol. 22, no. 10, pp. 12707–12715, May 2014.
[3] N. Xiang, Z. Zhang, J. Dang, and L. Wu, "A novel receiver design for PAM-DMT in optical wireless communication systems," *IEEE Photon. Technol. Lett.*, vol. 27, no. 18, pp. 1919–1922, Sep. 15, 2015.
[4] N. Fernando, Y. Hong, and E. Viterbo, "Flip-OFDM for unipolar communication systems," *IEEE Trans. Commun.*, vol. 60, no. 12, pp. 3726–3733, Dec. 2012.
[5] J. Armstrong and B. Schmidt, "Comparison of asymmetrically clipped optical OFDM and DC-biased optical OFDM in AWGN," *IEEE Commun. Lett.*, vol. 12, no. 5, pp. 343–345, May 2008.
[6] Y.-D. Zang, J. Zhang, and L.-H. Si-Ma, "Anscombe root DCO-OFDM for SPAD-based visible light communication," *IEEE Photon. J.*, vol. 10, no. 2, pp. 1–9, Apr. 2018.
[7] Q. Wang, C. Qian, X. Guo, Z. Wang, D. G. Cunningham, and I. H. White, "Layered ACO-OFDM for intensity-modulated direct-detection optical wireless transmission," *Opt. Express*, vol. 23, no. 9, pp. 12382–12393, May 2015.
[8] Y. Sun, F. Yang, and J. Gao, "Novel dimmable visible light communication approach based on hybrid LACO-OFDM," *J. Lightw. Technol.*, vol. 36, no. 20, pp. 4942–4951, Oct. 15, 2018.

[9] F. Yang, Y. Sun, and J. Gao, "Adaptive LACO-OFDM with variable layer for visible light communication," *IEEE Photon. J.*, vol. 9, no. 6, Dec. 2017, Art. no. 7907908.
[10] T. Wang, F. Yang, L. Cheng, and J. Song, "Spectral-efficient generalized spatial modulation based hybrid dimming scheme with LACO-OFDM in VLC," *IEEE Access*, vol. 6, pp. 41153–41162, Jun. 2018.
[11] B. Li, W. Xu, S. Feng, and Z. Li, "Spectral-efficient reconstructed LACO-OFDM transmission for dimming compatible visible light communications," *IEEE Photon. J.*, vol. 11, no. 1, Feb. 2019, Art. no. 7900714.
[12] X. Zhang, Q. Wang, R. Zhang, S. Chen, and L. Hanzo, "Performance analysis of layered ACO-OFDM," *IEEE Access*, vol. 5, pp. 18366–18381, 2017.
[13] W.-W. Hu, "PAPR reduction in DCO-OFDM visible light communication systems using optimized odd and even sequences combination," *IEEE Photon. J.*, vol. 11, no. 1, Feb. 2019. Art. no. 7901115.
[14] T. Zhang, J. Zhou, Z. Zhang, Y. Lu, F. Su, and Y. Qiao, "Dimming control systems based on low-PAPR SCFDM for visible light communications," *IEEE Photon. J.*, vol. 10, no. 5, Oct. 2018. Art. no. 7907211.
[15] T. Zhang, Y. Zou, J. Sun, and S. Qiao, "Improved companding transform for PAPR reduction in ACO-OFDM-Based VLC systems," *IEEE Commun. Lett.*, vol. 22, no. 6, pp. 1180–1183, Jun. 2018.
[16] B. Li, W. Xu, H. Zhang, C. Zhao, and L. Hanzo, "PAPR reduction for hybrid ACO-OFDM aided IM/DD optical wireless vehicular communications," *IEEE Trans. Veh. Technol.*, vol. 66, no. 10, pp. 9561–9566, Oct. 2017.
[17] Y. Xiao, M. Chen, F. Li, J. Tang, Y. Liu, and L. Chen, "PAPR reduction based on chaos combined with SLM technique in optical OFDM IM/DD system," *Opt. Fiber Technol.*, vol. 21, pp. 81–86, Jan. 2015.
[18] S. P. Valluri, V. Kishore, and V. M. Vakamulla, "A new selective mapping scheme for visible light systems," *IEEE Access*, vol. 8, pp. 18087–18096, 2020.
[19] W.-W. Hu, "SLM-based ACO-OFDM VLC system with low-complexity minimum amplitude difference decoder," *Electron. Lett.*, vol. 54, no. 3, pp. 144–146, Feb. 2018.
[20] D. Xin, Q. Xu, S. Qiao, and T. Zhang, "Non-linear companding transform for DCO-OFDM-based VLC systems," *IET Commun.*, vol. 13, no. 8, pp. 1110–1114, May 2019.

WEIWEN HU (Member, IEEE) received the B.S. degree in electrical engineering from National Chung Cheng University, Chia-Yi, Taiwan, in 2003, and the M.S. degree in communications engineering and the Ph.D. degree in electrical engineering from National Sun Yat-Sen University, Kaohsiung, Taiwan, in 2005 and 2012, respectively.

From 2005 to 2012, he was an Associate Engineer with the Environment Control and Network Technology Department, Industrial Technical Research Institute. From 2013 to 2015, he was the Principal Engineer with the Department of Electrical, Radiant Opto-Electronics Corporation. In 2015, he joined the Department of Electronic Engineering, Southern Taiwan University of Science and Technology, Taiwan. His research interests include wireless communication systems, communication sequences design, optical wireless communication, OFDM, and digital signal processing. He also served as a TPC member and reviewer for many IEEE international conferences and journals. He is currently an Associate Editor of IEEE Access.